Am J Transl Res 2019;11(11):6907-6923
www.ajtr.org /ISSN:1943-8141/AJTR0099204

*Original Article*

# Multiplexed detection and the establishment of a novel high-throughput method for human germ cell quality screening based on aggregation-induced emission

Zixuan Zeng[1], Xiaojiao Ren[1], Tailang Yin[2], Xiang Gao[2], Mengting Tsai[1], Yi Zhang[1], Meijia Gu[1]

[1]*Key Laboratory of Combinatorial Biosynthesis and Drug Discovery, Ministry of Education, School of Pharmaceutical Sciences, Zhongnan Hospital, Wuhan University, Wuhan 430071, Hubei, China;* [2]*Reproductive Medicine Center, Renmin Hospital of Wuhan University, Wuhan 430060, Hubei, China*

Received July 3, 2019; Accepted November 2, 2019; Epub November 15, 2019; Published November 30, 2019

**Abstract:** We report a rapid, sensitive, and high-throughput method for quality control of human sperm cells and oocytes staining based on the aggregation-induced emission feature of the tetraphenylethylene-based luminogen (TPE-Ph-In), which is mitochondria-specific. Germ cells are evaluated to assess fertility and to facilitate assisted reproduction. In regular clinical practice, sperm quality is determined on the basis of visual examination and mathematical models of the sperm cell number, motility, and morphology. The maturation of the oocyte is crucial for the developmental competence of the resulting embryo. Human *in vitro* fertilization (IVF) have indicated that delaying insemination improves fertilization rates, presumably by allowing the completion of cytoplasmic maturation for those oocytes that have not completely matured at the time. Therefore, a more reliable method to determine germ cell quality is needed. The mitochondrial membrane potential (MMP) of spermatozoa reflects the function and status of those cells. In oocytes, the distribution of mitochondria indicates the readiness of the cell for fertilization. Aggregation-induced emission luminogens (AIEgens) have good biocompatibility and photostability and produce low levels of background signal. There are about 100,000 mitochondria per fully-grown human oocyte. Mitochondria in mammalian oocytes are spherical with little cristae, supplying large scale of ATP for embryo development. Here, we expanded the use of TPE-Ph-Into determine germ cell quality on the basis of the MMP and the intracellular distribution of mitochondria. We stained clinical sperm samples from 36 patients with infertility, as well as four oocytes, with TPE-Ph-In and examined the cells by confocal microscopy and cell sorting analysis. Our results showed a positive correlation between the MMP and sperm cell motility, as well as the different distribution of mitochondria in oocyte. Thus, staining with TPE-Ph-In could be used to quickly determine germ cell quality *in vivo*, bringing new possibilities for applications of AIEgens in biomedical research and clinical trials.

**Keywords:** Aggregation-induced emission (AIE), tetraphenylethylene (TPE), human germ cell quality

## Introduction

Failed fertilization happens in infertility and may result from defective spermatozoa and/or oocytes. Individuals with poor germ motility are usually infertile unless require assisted reproductive techniques are to achieve successful fertilization employed. Infertility is a global health issue affecting 48.5 to 186 million couples worldwide, with 20-70% of the cases being attributable to male factors 1. Numerous clinical studies confirmed the existence of paternal contributions to faulty fertilization and aberrant embryo development [1-4], highlighting the need to select the best sperm cells before *in vitro* fertilization (IVF) is attempted. Routine clinical tests to evaluate sperm characteristics include numeration and determination of motility, vitality, and morphology. The current methods of semen quality analysis have limited clinical value for predicting IVF success, with a success rate of less than 50% [5]. In clinic, when the oocyte was subjected to ICSI, it was regularly observed just under an inverted microscope. The density of the central region and the whole size of the oocyte was observed [6]. Thus poor-quality oocytes are another factor that limits reproductive success [7]. Despite significant improvements in implantation and pregnancy rates over the years, 60% of fresh embryos with

acceptable morphology fail to implant because of mitochondrial defects or chromosomal anomalies [8, 9]. In addition, there is a critical age-dependent decline in the quality of oocytes [10]. Better methods to determine germ cell quality are required, which will make it possible to exclude useless *in vitro* fertilization attempts.

Mitochondria play crucial roles in cellular energy metabolism and tightly regulate cellular homeostasis, viability, and physiological functions [11]. Many factors can alter the mitochondria, leading to mitochondrial dysfunction or even neurodegenerative and cardiovascular diseases [12-14]. Mitochondria supply energy to cells through a series of biochemical processes [11] in which free energy is released from nutrients and channeled by the respiratory chain to generate an electrochemical gradient across the inner mitochondrial membrane called the mitochondrial membrane potential (MMP), which is used by ATP-synthase to generate ATP.

Mitochondria play vital roles in oocyte functions during preimplantation embryonic development, as glycolysis is limited after fertilization and mitochondrial replication is suppressed from metaphase-II until the hatched blastocyst stage [15]. Mitochondria possess their own small genome and are inherited uniparentally from the mother, as sperm mitochondrial proteins are ubiquitinated and degraded after the sperm cell gains entry into the oocyte [16-19]. Dysfunction of oocyte mitochondria is believed to be a key factor in poor developmental competence of oocytes in older females [20]. High ATP levels in oocytes correlate with better embryo development and implantation rates [21]. Attenuated mitochondrial activity reduces the production of ATP, and failure of ATP production has been shown to have deleterious consequences on chromosome segregation and embryonic development [22]. Long-term observation of mitochondrial dynamics in oocytes is difficult, because the fluorescence intensity of commercially available mitochondria-specific markers rapidly decreases.

Mitochondria are one of the most important determinants of male fertility, playing a crucial role in sperm motility, hyper activation, capacitation, and fertilization. The activated motility of ejaculated spermatozoa and the hyperactivated motility of spermatozoa during fertilization both require a sufficient supply of energy. In sperm cells, mitochondria are exclusively confined to the mitochondrial capsule, which is located in the sperm mid-piece and wrapped tightly around the axoneme. Because of their tight packing and strict localization in the mitochondrial capsule, sperm mitochondria are difficult to isolate using conventional separation methods [23]. It has been proposed that the MMP across the inner mitochondrial membrane of human spermatozoa is an indicator of sperm quality [24-26]. Abnormal MMP in sperm mitochondria may lead to mitochondria dysfunction, resulting in male infertility [27].

The measurement of MMP using potentiometric dyes is considered to be a reliable test to determine germ cell quality. Several fluorescent probes have been developed to image mitochondria in living cells, such as rhodamine 123 (Rh 123) and JC-1 cationic groups [28-30]. Those fluorochromes accumulate preferentially in hyperpolarized mitochondria, which have a high membrane potential, allowing those mitochondria to be distinguished from depolarized mitochondria, which have a low membrane potential [31]. Rh 123 and JC-1 both suffer from limitations including high cytotoxicity, low selectivity, and poor photostability due to the aggregation-induced emission-quenching (ACQ) effect, even at very high concentrations. A previous study reported on the complexities and false results associated with the use of JC-10 to measure MMP [31]. The fluorescence emission of JC-1 is limited, making errors difficult to predict. For the monitoring of germ cell quality in clinical applications, luminogens need to have low cytotoxicity and high photostability, and the fluorescence quantum yield should be as strong as possible to achieve accuracy for long-lasting tracking. Therefore, the use of ACQ dyes to track MMP is not suitable for clinical tests of germ cell quality.

In 2001, the unique photophysical phenomenon of aggregation-induced emission (AIE) was discovered [32]. Luminogens with AIE (AIEgens) are almost nonfluorescent in the solution state but become highly emissive when aggregates are formed. The major mechanism of AIE is the restriction of intramolecular rotation [33]. AIEgens display strong fluorescence and good photostability [33-35]. Researchers have already started to explore the applications of AIE

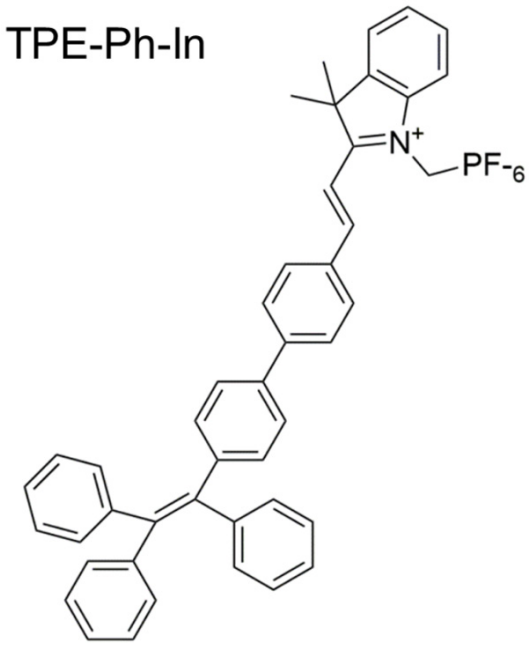


**Scheme 1.** Structures and emission spectra of TPE-Ph-In in DMSO and DMSO/water mixtures with 99% water fractions (*f*w). Dye concentration: 10 mM; excitation wavelength: 450 nm. Inset: photographs of TPE-Ph-In in DMSO/water mixtures with *f*w values of 0% and 99% under 365 nm UV irradiation. (redrawn from [38]).

probes in a variety of biological and medical applications [36-39]. Tetraphenylethylene (TPE) derivatives are the most widely used AIEgens, because they are stable and easy to synthesize. Recently, Tang et al. examined a series of TPE derivatives using ultrafast spectroscopy and confirmed that central C = C bond elongation and p twist after photoexcitation was the main cause of non-radiative decay [40]. TPE-Ph-In, the first non-self-quenching mitochondria-specific probe, was synthesized by incorporating indolium salt into TPE (**Scheme 1**) [38]. With high sensitivity to intramolecular charge transfer, normally based on donor-acceptor architecture, TPE-Ph-In is widely used as a red emitter [41-43]. The indolium salt in TPE-Ph-In is positively charged and serves as an electron-accepting moiety for mitochondrial targeting [44-46]. TPE-Ph-In is non-emissive in solution, but when it accumulates in mitochondria its fluorescence signal is switched on because of the aggregation of the TPE residues. TPE-Ph-In can easily penetrate the cell membrane and access the mitochondria, which ensures its high sensitivity for *in situ* imaging of the MMP. Because of its good photostability, excellent biocompatibility, and high signal-to-noise ratio, TPE-Ph-In has proven useful for monitoring biological processes *in vitro* [38, 47-49]. Moreover, TPE-Ph-In not only targets mitochondria but also can be used to monitor changes in MMP [50, 51]. As such, the superior performance of TPE-Ph-In has motivated us to exploit it *in vivo* for (pre) clinical investigation.

In this study, we demonstrate the development of a novel method to evaluate germ cell quality on the basis of real-time monitoring of MMP. Fluorescence microscopy, flow cytometry, and computational analysis techniques are widely applied to evaluate germ cell characteristics [52]. We used TPE-Ph-In and Hoechst 33342 staining together with flow cytometry analysis to examine the quality of semen samples from 36 men with infertility. We also used TPE-Ph-In and Hoechst 33342 staining to evaluate the status of four abandoned oocytes. The evaluation of germ cell quality using TPE-Ph-In staining and flow cytometry requires smaller samples and less time than conventional analyses and is accurate and suitable for high-throughput, multiplexed assays. This method can be used to determine the sperm quality in about 1 h, providing information on sperm concentration, morphology, and MMP. On the other hand we also staining the oocyte and obverse using the confocal microscope, which could help us finish the morphology assessment and MMP detection at the same time

## Results

### *Cytotoxicity test of TPE-Ph-In*

Dyes used in image analyses of living cells must have low cellular toxicity. We therefore evaluated the cytotoxicity of TPE-Ph-In in HeLa and HCT 116 cells using a 3-(4,5-dimethyl-2-thiazolyl)-2,5-diphenyltetrazolium bromide (MTT) assay. Both cell types maintained high viability (≥90%) after treatment with 10 μM (an appropriate concentration for imaging) TPE-Ph-In for 0.5 h, 1 h, or 1.5 h (Figures S1 and S2). We also measured the physiological characteristics of sperm cells after staining with TPE-Ph-In under the same conditions (**Table 1**). There was almost no change in progressive motility and non-progressive motility after the cells were stained and scanned.

**Table 1.** Sperm characteristics of semen and prepared spermatozoa

| | No. of samples | Mean (SEM) | Minimum | Median | Maximum |
|---|---|---|---|---|---|
| Sperm concentration (× $10^6$/ml) | 36 | 79.9±8.15 | 9.5 | 80.1 | 272.5 |
| Progressive (PR) motility in neat semen (%) | 36 | 32.3±2.5 | 2 | 31.5 | 61.4 |
| Non-Progressive (NP) motility in neat semen (%) | 36 | 20.9±1.4 | 5.2 | 18.8 | 35.7 |
| RP+NP | 36 | 53.2±3.3 | 7.6 | 56.2 | 86.9 |
| Normal morphology (%) | 36 | 7.4±0.28 | 4 | 7 | 15 |

All of the 36 samples came from Renmin Hospital of Wuhan University from April to May 2019. The data of Patient sample is from XJB.

*Imaging of sperm cells stained by TPE-Ph-In*

We performed a colocalization experiment using TPE-Ph-In and the mitochondria-specific dye MitoTracker Green in HeLa cells. The results showed that TPE-Ph-In localized in the same locations as MitoTracker Green (Figure S1A), indicating that TPE-Ph-In localized specifically in the mitochondria. To confirm whether TPE-Ph-In has the capability to indicate alterations in MMP, we pretreated HeLa and HCT 116 cells with carbonyl cyanide m-chlorophenylhydrazone (CCCP), a mitochondrial uncoupler, in order to change the MMP during the staining process. CCCP promotes the release of intra-mitochondrial cations and causes rapid acidification by collapsing the MMP [53]. We found that TPE-Ph-In could quickly penetrate untreated cells and accumulate in the mitochondria to give a bright red fluorescence (Figure S1C). The fluorescence signal of TPE-Ph-In can directly represent the MMP on the basis of the positive correlation between the fluorescence intensity and the local dye concentration in the mitochondria [38, 47], which is difficult to achieve for traditional dyes suffering from ACQ effects [38, 47]. The CCCP treatment led to a decrease in the intensity of the red fluorescent signal of the TPE-Ph-In, reflecting the CCCP-induced decline in the MMP.

*Real-time in vivo bioimaging of human sperm cells*

We incubated human sperm samples with 10 mM TPE-Ph-In and 1 μg/ml Hoechst 33342 (Sigma-Aldrich, 861405) for nuclear staining for 0.5 h. The motion of the sperm cells stained with TPE-Ph-In and Hoechst 33342 is shown in Video S1. The fluorescence intensity in the TPE-Ph-In-stained mitochondria was a good indicator of the level of sperm motility, suggesting that TPE-Ph-In can be used to monitor the activity of sperm cells. To gain further understanding about it, the dynamic motion of clinical sperm cells were stained with TPE-Ph-In was tracked and recorded (Video S1). **Figure 1** shows the merged TPE-Ph-In and Hoechst 33342 staining of representative sperm cells. The results confirmed that the mitochondria were localized in the spermatozoa mid-piece. TPE-Ph-In could thus specifically bind negatively charged mitochondria and indicate the mitochondria membrane potential changes in living cells [38]. The excitation wavelength of TPE-Ph-In was 561 nm, and a lambda scan showed that a strong emission occurred at 596-663 nm (**Figure 4**). The detailed imaging results for all of the 36 patients' samples are given in the supporting information.

The imaging results revealed that energetic sperm cells produce bright red fluorescence with TPE-Ph-In staining comes from the energetic sperms, while the inactive sperm cells give only give faint red fluorescence or even do not given fluorescence at all. It has been known that Mitochondria of spermatogenic cells modify their morphological organization, number, and location. Mitochondria, localized in the mid-piece area of sperm flagellum, produce ATP to support sperm motility, as a key indicator of sperm function. Mitochondria in mature spermatozoon spermatids aggregate and form the mitochondrial sheath of the middle piece [54, 55]. There is a good correlation between the MMP$\Delta\psi_m$ and overall fertilizing capability of a subpopulations of human spermatozoa showing the highest better fertilization potential is are characterized by a high mitochondrial functionality, as detected with mitochondrial probes [56]. In our results, the mid-pieces of sperms presented various degrees of fluorescence intensity, as shown in Video S1, strong fluorescence signals were observed appeared in the middle- pieces of living sperm cells with high vitality. Interestingly, we also found that some fewer active sperm cells displayed fluorescence were near the head of spermregion. Typical morphological

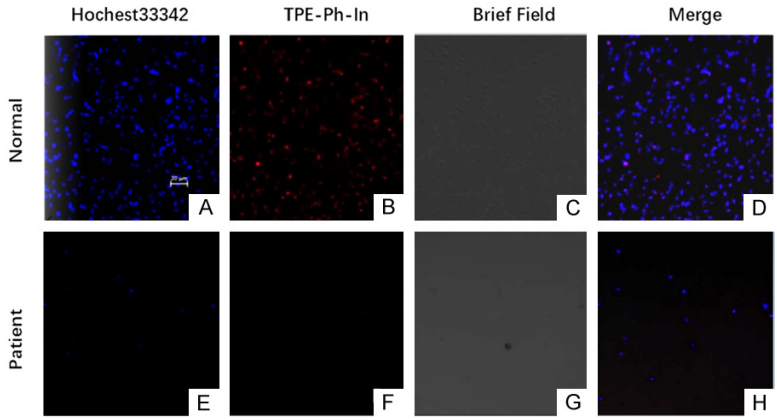


**Figure 1.** The staining of clinical sperm samples from an individual with normal fertility and a patient with infertility. The sperm cell concentration is higher in the sample from the individual with normal fertility than in the sample from the patient with infertility. The tails of the sperm cells are stained red by TPE-Ph-In. Scale bar = 20 μm. A-D. The sperm cells of an individual with normal fertility stained with TPE-Ph-In (red) and Hoechst 33342 (blue). E-H. The sperm cells from patients stained with TPE-Ph-In (red) and Hoechst 33342 (blue). Normal control is from ZS. Patient sample is from LP.

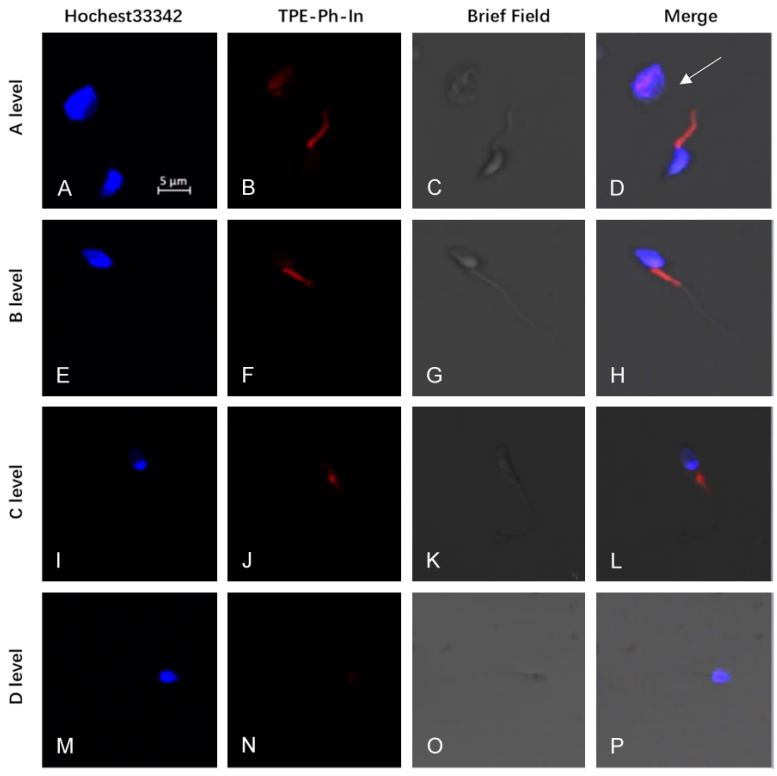


**Figure 2.** Confocal images of four different grades of sperm cells from patients' samples stained with TPE-Ph-In (red) for 30 min. Blue signal indicates the cell nucleus stained by Hoechst 33342. Red signal indicates mitochondria stained by TPE-Ph-In. The white arrow points out deformed sperm without a tail. Excitation wavelength: 561 nm, emission wavelength: 596-663 nm (for TPE-Ph-In); excitation wavelength: 405 nm, emission wavelength: 410-531 nm (for Hoechst 33342). Scale bar = 5 μm.

signs of apoptosis include plasma membrane blebbing with the formation of apoptotic bodies, impaired mitochondrial integrity, defects of the nuclear envelope, and nuclear fragmentation. All of those; these morphologies signs have also been observed in human sperm cells. Increased membrane permeability of spermatozoa is a sign of early apoptosis in spermatozoa [57, 58]. Compared to with their immature counterparts, mature sperm cells showed signs of apoptosis less frequently. In particular, their mitochondria were more intact, the nucleus was minimally fragmented, and nuclear envelope defects were rarely observed [59]. Assays capable to of detecting apoptotic spermatozoa can identify defective spermatozoa at an early stage of damage and thus can be better assays of sperm quality [60, 61]. Hereby our findings further the great value of this technique for sperm analysis.

Human sperm preserves a number of mitochondria in a specific subcellular compartment, indicating that the functionality of these organelles might be crucial. In addition, sperm mitochondria become polarized, and thus functional. Likewise, a remarkable change in human sperm mitochondria towards a more loosely wrapped morphology, possibly resulting from an increase in mitochondrial volume, was associated with capacitation [62]. Asthenozoospermia is a fertility-impairing pathology linked to a more or less pronounced reduction of

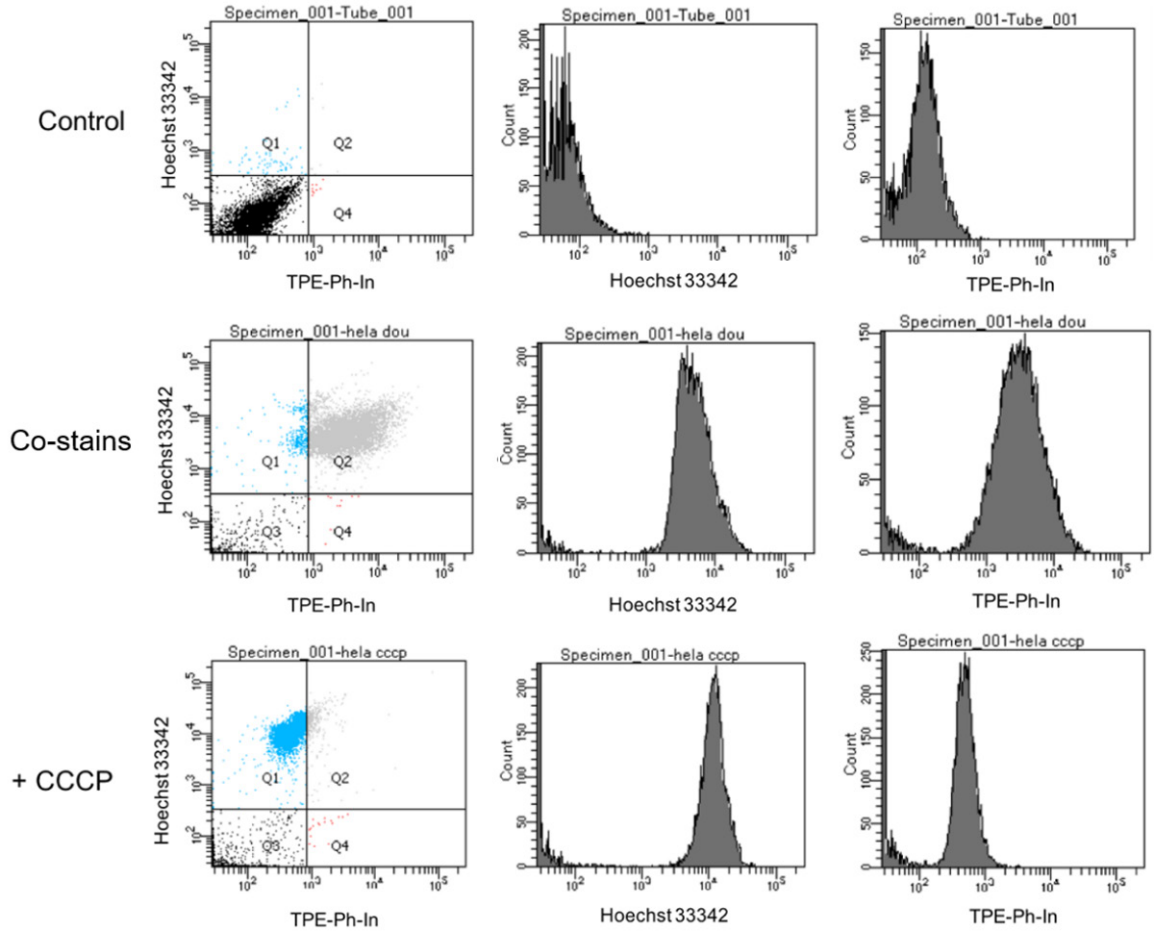


**Figure 3.** Co-staining of HeLa cells with Hoechst 33342 (blue) and TPE-Ph-In (red). The untreated cell membrane potential with co-staining is normal, with the cell population mostly gathered in the Q2 region and strong signals in both the red and the blue channels (red channel: photoluminescence = 4043; blue channel: photoluminescence = 5669). After the cells were treated with carbonyl carbonyl cyanide 3-chlorophenylhydrazone (CCCP), the red fluorescence almost disappeared, whereas the blue fluorescence intensity did not change (red light: 462 blue light: 11234). The results indicate that the state of the cell membrane potential can be accurately judged by the change in the intensity of red fluorescence. Scale bar = 10 μm.

sperm motility. Structural alterations of sperm flagella are responsible for reduced motility in asthenozoospermic infertile men. By electron microscopic analysis of semen samples, defects in the components of the periaxonemal structures, mitochondrial helix and fibrous sheath, can be recognized [63].

Abnormalities of mitochondrial organization include a shorter mid-piece with fewer mitochondrial gyres, total absence of mitochondria from the mid-piece, lack of the mid-piece segment, bad assembly or clustering of mitochondria with normal ultrastructure [64, 65]. In some cases of asthenozoospermia, sperm mitochondria can be functionally active and present a high $\Delta\psi_m$ in a large number of cells. Therefore, the low sperm motility does not necessarily result from energetic disturbances of sperm mitochondria, but it may be associated with deformations of the mitochondrial sheath containing functional mitochondria [66].

*Imaging of four different grades of clinical sperm samples*

We chose four clinical grades of sperm from patients to show the detailed differences among the grades. As shown in **Figure 2**, white arrowhead points out the sperm with deformity tail. Even without any red fluorescence, the shape of this sperm is not clear in the bright field. Fast-moving sperm with a Z-shaped tail are shown in **Figure 2B-F**. The average fluorescence intensity of those sperm cells is greater than 35. **Figure 2I-P** shows moving sperm with

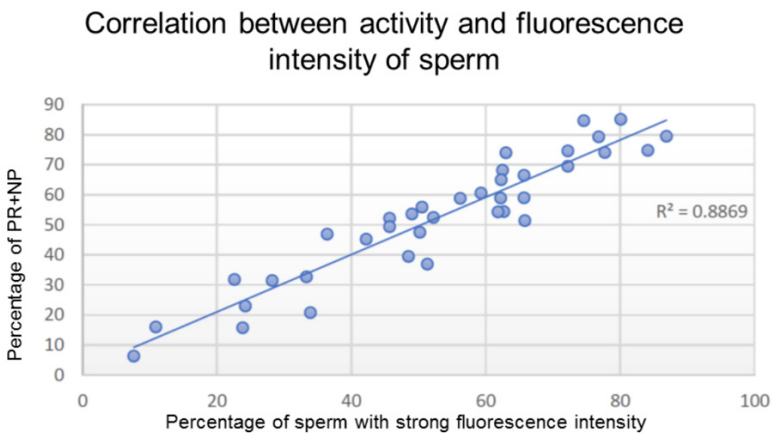


**Figure 4.** Correlation between conventional sperm analysis (progressive + nonprogressive motility) and flow cytometry results of 36 patients' sample. The correlation coefficient is $R^2 = 0.8869$. All flow cytometry results for patients are included in the Supplementary File. $P < 0.05$ was considered statistically significant.

a straight tail and an average fluorescence intensity of 42. There were differences in sperm reactivation and MMP between fast-moving and slow-moving sperm cells. By staining the sperm with TPE-Ph-In as well as Hoechst 33342, we could identify more active sperm from the semen samples. The percentages of Grade A and Grade B spermatozoa in our 36 samples from patients were < 50% and < 25%, respectively.

In clinic, the motility of sperm is divided into four different grades: Grade A (also denoted motility IV): Sperm with progressive motility. These are the strongest and swim fast in a straight line. Grade B (also denoted motility III): (non-linear motility): These also move forward but tend to travel in a curved or crooked motion. Grade C (also denoted motility II): These have non-progressive motility because they do not move forward despite the fact that they move their tails. Grade D (also denoted motility I): These are immotile and fail to move at all. Spermatozoa with rapid forward movement and Grade b with slightly slow forward movement (A + B) were less than 50% or 25% respectively. (1) Mild asthenospermia refers to Grade A + B sperm < 50%, but > 30% or grade a sperm < 25%, but > 10%. Secondly, moderate asthenospermia refers percentage of Grade A sperm cells is below 10%. Severe asthenospermia is when Grade B and Grade C sperm cells make up less than 30% of the total sperm population, and the population contains no Grade A sperm cells. I mild asthenospermia refers to a Grade B sperm < 50%, but > 30% or A Grade sperm < 25%, but > 10%, II moderate asthenospermia refers to a Grade B sperm < 50%, but > 30%. Grade A spermatozoa < 10%, III severe asthenospermia refers to the number of Grade B and C spermatozoa < 30%, among which Grade A spermatozoa is zero.

*Flow cytometry analysis of sperm*

We performed flow cytometry analysis of samples of TPE-Ph-In-stained HeLa cells and sperm cells to evaluate the average MMP of the samples. Cells without any treatment served as a blank control, showing only the autofluorescence originating from the cells (**Figure 3**). We incubated the cells with TPE-Ph-In at 37°C for 0.5 h. The results of prior conventional analysis of the sperm samples to determine the numbers of cells with progressive and non-progressive motility correlated strongly with the average MMP values determined by flow cytometry ($R^2 = 0.8869$; **Figures 3** and **4**). The results of the flow cytometry analysis of the 36 patients' samples are given in the supporting information.

*Photostability of TPE-Ph-In in live sperm cells*

The intracellular fluorescence of TPE-Ph-In changed only slightly, even after constant laser irradiation under a confocal fluorescence microscope for 360 s (Figure S2). Confocal images of sperm cells stained with TPE-Ph-In taken under continuous excitation at 561 nm for 30 scans within 360 s photoluminescence (PL = 78.829) showed that the fluorescence intensity of TPE-Ph-In declined by only 8% as the number of scans increased, demonstrating that TPE-Ph-In possesses strong photostability and high resistance to photobleaching. Our results suggest that TPE-Ph-In is applicable for *in vivo* time-lapse and long-term bioimaging studies of sperm cells.

*High-throughput method acquisition*

Fast imaging with a confocal microscope of 10 clinical semen samples provided information about sperm concentration and morphology. Analysis of the images shown in **Figure 5A**. The

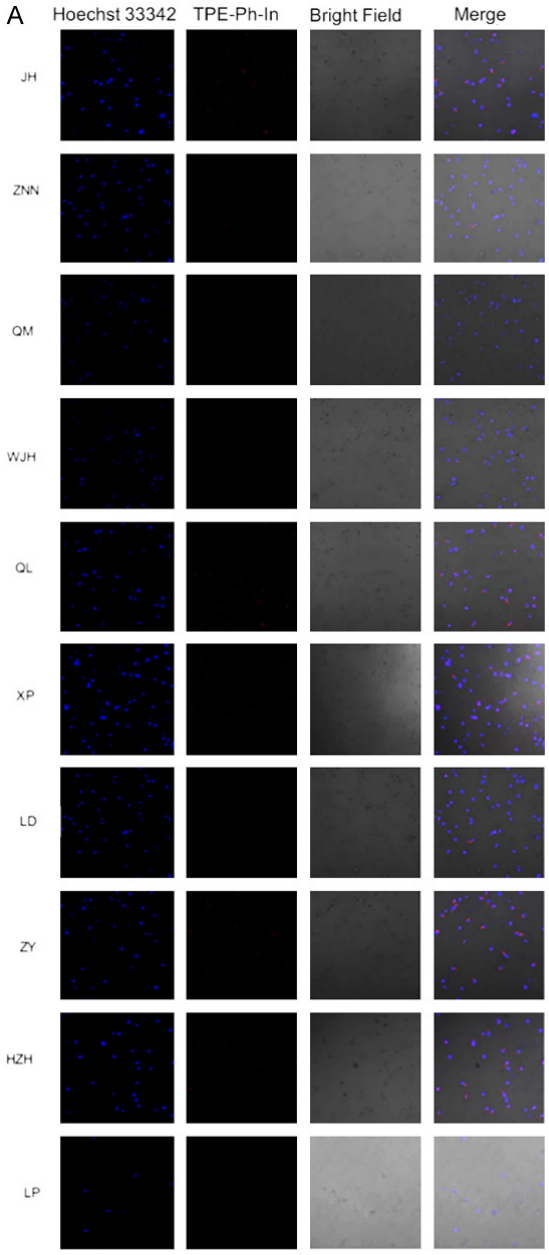


B

| Patient Name | Sperm Number % | PL intensity | PR+NP |
|---|---|---|---|
| JH | 41.3 | con | 51.3 |
| ZNN | 16 | 28.4 | 22.6 |
| QM | 7.2 | 19.1 | 10.9 |
| WJH | 31 | 38.5 | 36.4 |
| QL | 47 | 56.1 | 50.5 |
| XP | 22.9 | 32.2 | 28.2 |
| LD | 17.6 | 27.5 | 23.8 |
| ZY | 44.4 | 67.5 | 48.5 |
| HZH | 37 | 43.75 | 33.3 |
| LP | 5.6 | 14 | 7.6 |

C

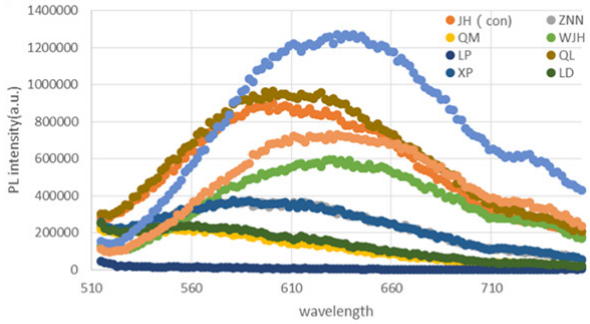


**Figure 5.** Establishment of a high-throughput method to determine sperm quality. A. Fast imaging for the sperm cells in clinical samples stained with TPE-Ph-In (red) and Hoechst 33342 (blue) after regular pretreatment, detailed described in material and methods. Scale bar = 20 μm. B. The sperm cell concentrations of the tested samples. C. Photoluminescence spectra of clinical samples stained with TPE-Ph-In and Hoechst 33342. Normal control is from ZS.

sperm cell concentrations of the tested samples, as shown in **Figure 5B**. We next measured the fluorescence spectra of TPE-Ph-In in eight (8/36, 22%) randomly selected clinical semen samples. The differences between samples from individuals with normal fertility and patients with infertility showed that the TPE-Ph-In fluorescence intensity was indicative of the magnitude of the MMP. When sperm cells are introduced into this system, the solution shows strong red fluorescence the excitation wavelength is 561 nm. Previous results showed that the excitation wavelength of TPE-Ph-In is 450 nm [38]. The photoluminescence spectra of TPE-Ph-In in buffer solutions with different clinical semen samples are shown in **Figure 5C**. Notably, in the presence of sperm cells, the fluorescence intensities of TPE-Ph-In in the different clinical semen samples were also enhanced, which may be attributed to the AIE feature of TPE-Ph-In. TPE-Ph-In is not water soluble but has good water miscibility. Upon binding to mitochondria, the intramolecular motion of TPE-Ph-In is restricted further, which leads to fluorescence enhancement. The fluorescence intensity of the solution appeared at 615 nm and 480 nm. Identical acquisition settings, including laser intensity and exposure time, were used for each well on the same plate, which made it easy to count the numbers of

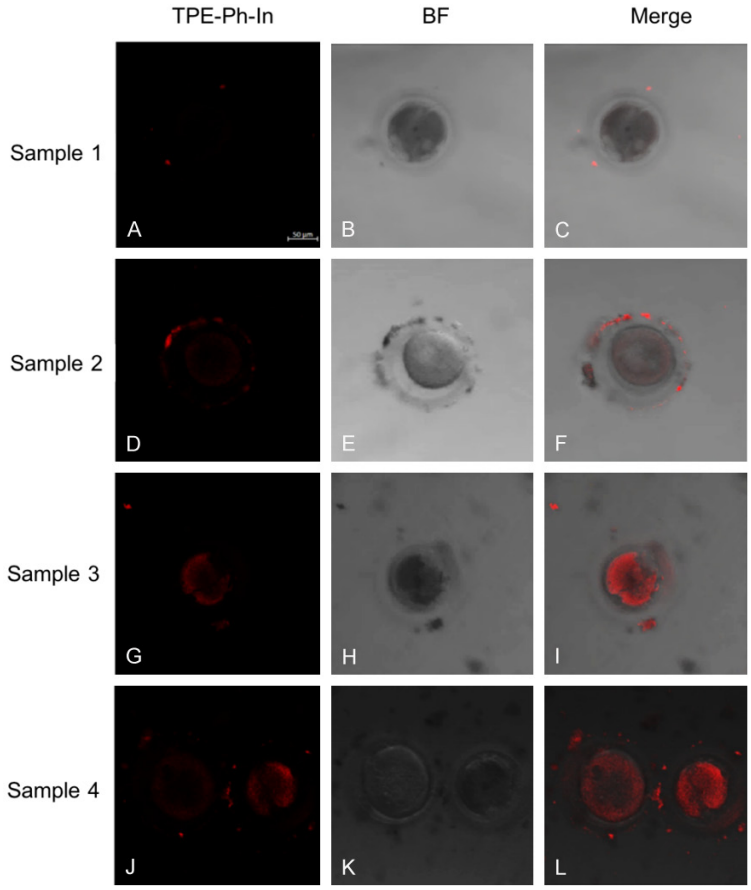


**Figure 6.** Confocal microscopy imaging of mitochondria in a human oocyte. Clinical sample 1 and Clinical sample 2 are from live oocytes in metaphase-II. Clinical sample 3 and Clinical samples 4 are from live oocytes in the germinal vesicle stage.

functional mitochondria and to observe the sperm cells in real time.

*Real-time imaging of mitochondria in human oocytes*

The mammalian oocyte typically contains about 100,000 mitochondria that can occupy up to 30% of the cytoplasmic space [67]. The quality of oocytes is critically associated with mitochondrial dysfunction. Most oocytes retrieved from ovaries are mature, metaphase-II-arrested oocytes, but about 10-20% remain immature, at metaphase-I or prophase-I (germinal vesicle stage). The recognition of oocyte maturation arrest as a specific condition may contribute to the characterization of what is currently known as the "oocyte factor". Oocyte maturation is the breakdown of the germinal vesicle in prophase-I oocytes and subsequent completion of meiosis-I and meiosis-II in the ovarian follicle. Studies of oocyte maturation have mainly focused on molecular processes [68-72] and gene-expression profiles [73]. There are few data on the ultrastructural analysis of immature or mature human oocytes. Such data would shed light on the cellular mechanisms that underlie oocyte maturation, which are important for the establishment of optimal *in vitro* handling protocols for oocytes after follicle retrieval for IVF. The redistribution of mitochondria is an important event in oocyte maturation, and the mitochondrial distribution is considered a marker of oocyte cytoplasmic maturity [74-81]. Mammalian oocytes have more mitochondria and greater cytoplasmic volume than somatic cells [82]. Mitochondria disperse homogeneously throughout the cytoplasm with concomitant disappearance of the aggregated structure just after germinal vesicle breakdown. Mitochondria in metaphase-I oocytes localize around the spindle and form large clusters [80]. The oocyte size and mitochondria rearrangement around the nucleus are associated with the oocyte's potential to resume meiosis *in vitro* [83]. It is difficult to obtain precise information about the dynamics of mitochondria in mammalian oocytes. The mitochondrial distribution in human oocytes is defined as peripheral (located largely in the cortical region of the oocytes), diffuse (spread evenly over the cytoplasm), or semi-peripheral (between peripheral and diffused distribution) [75]. Normally, the mitochondrial distribution in human metaphase-I oocytes is considered to be peripheral or semi-peripheral and diffuse [84].

We obtained four clinical oocyte samples and stained them with TPE-Ph-In, followed by confocal imaging. The oocytes had small numbers of mitochondria, which were not dispersed homogeneously throughout the cytoplasm with concomitant disappearance of the aggregated structure (**Figure 6**). Also, the TPE-Ph-In fluorescence was very weak, indicating a low level of mitochondrial activity. The clinical oocyte sam-

ples 3 and 4 were from the germinal vesicle stage. As shown in **Figure 6**, we found that the mitochondria were distributed throughout the whole oocyte, with high MMP.

## Discussion

Infertility is a global health issue affecting 48.5 to 186 million couples worldwide, with 20-70% of the cases being attributable to male factors [85]. Our imaging results revealed that energetic sperm cells produce bright red fluorescence with TPE-Ph-In staining, whereas inactive sperm cells give only faint red fluorescence or no fluorescence at all. Mitochondria of spermatogenic cells modify their morphological organization, number, and location. Mitochondria in mature spermatids aggregate and form the mitochondrial sheath of the mid-piece [54, 55]. The MMP is correlated with the overall fertilization capability of spermatozoa in human sperm samples [86]. Furthermore, subpopulations of human spermatozoa showing the highest fertilization potential are characterized by high mitochondrial functionality, as detected by mitochondrial probes [56]. In our results, the mid-pieces of sperm cells presented various degrees of fluorescence intensity. We also found that some active sperm cells displayed fluorescence near the head region. Typical morphological signs of apoptosis include plasma membrane blebbing with the formation of apoptotic bodies, impaired mitochondrial integrity, defects of the nuclear envelope, and nuclear fragmentation. All of those signs have been observed in human sperm cells. Increased membrane permeability of spermatozoa is a sign of early apoptosis [57, 58]. Compared with their immature counterparts, mature sperm cells show signs of apoptosis less frequently; their mitochondria are more intact, the nucleus is minimally fragmented, and nuclear envelope defects are rarely observed [59]. Assays capable of detecting apoptotic spermatozoa can identify defective spermatozoa at an early stage of damage [60, 61].

Sperm mitochondria become polarized and thus functional. Accordingly, a remarkable change in human sperm mitochondria toward a more loosely wrapped morphology, possibly resulting from an increase in mitochondrial volume, is associated with capacitation [62]. Asthenozoospermia is a fertility-impairing pathology linked to a more or less pronounced reduction of sperm motility. Structural alterations of sperm flagella are responsible for reduced motility in asthenozoospermic infertile men. Electron microscopic analysis of semen samples can identify defects in the components of the periaxonemal structures, mitochondrial helix, and fibrous sheath [63]. Abnormalities of mitochondrial organization include a shorter mid-piece with fewer mitochondrial gyres, a total absence of mitochondria from the mid-piece, a lack of the mid-piece segment, and bad assembly or clustering of mitochondria with normal ultrastructure [64, 65]. In some cases of asthenozoospermia, sperm mitochondria can be functionally active and present a high MMP in a large number of cells. Therefore, the low sperm motility does not necessarily result from energetic disturbances of sperm mitochondria, but may instead be associated with deformations of the mitochondrial sheath containing functional mitochondria [66].

Because of the complexity of the problem, the goal of developing assays that accurately predict the fertilization capacity of semen samples has not yet been achieved. The percentage of motile sperm in a clinical sample is the most commonly used measure to evaluate semen quality, but that measure is not highly correlated with the fertilization capacity of semen samples. New laboratory assays are being developed to evaluate the fertilization ability of sperm. It is possible to obtain a better prediction of the fertilizing potential of a semen sample by using data from multiple sperm assays. Any laboratory measuring a single sperm attribute, motility for example, will produce results that do not correlate well with fertility, leading to failure of assisted reproductive techniques such as IVF and intracytoplasmic sperm injection.

TPE-Ph-In specifically targets mitochondria and has low cytotoxicity and high photostability, suggesting that it can be useful for bioimaging applications. Even after continuous irradiation, TPE-Ph-In could still easily penetrate cells and give stable fluorescence, making it an ideal candidate for biological applications requiring a long time. The turn-on signature of AIEgens is still not fully developed for *in vivo* applications, because most previous studies of AIEgens were performed *in vitro*, and the *in vivo* environment is much more complex. It is urgent to

make full use of the AIE mechanism for *in vivo* applications, especially in the clinical setting.

TPE-Ph-In contains a phenyl ring and has a strong AIE effect and good biocompatibility. Because of its cationic and lipophilic features, TPE-Ph-In localizes in the mitochondria in several cell lines and is sensitive to changes in the MMP, potentially making it widely useful to many biological and medical fields. Without the interference caused by the concentration-quenching problem, the fluorescence signal of TPE-Ph-In can directly represent the MMP. Our *in situ* application of TPE-Ph-In to detect the MMP in multiplexed detection assays using confocal microscopy and flow cytometry analysis produced results in agreement with those of conventional semen tests, demonstrating its great potential for probing and tracing the MMP and evaluating sperm vitality. Furthermore, we successfully developed a novel assay employing TPE-Ph-In to monitor sperm quality in a fluorescence "turn-on" manner. The assay is a simple and economical method for sperm quantification in aqueous media. The fluorescence signal approached a steady value after about 60 min. The quantification of sperm was highly sensitive. The system showed little response to various potential interfering substances and could still detect l-lactate with high sensitivity in systems with high protein content, although minor correction using a new calibration was necessary. Our high-throughput method can be performed with a commercially available setup and can be carried out continuously with volumes of semen as low as 120 μL. Furthermore, we used TPE-Ph-In to analyze mitochondrial dynamics in maturing oocytes. Thus, our method permits the examination of the pathophysiology of mitochondria in oocytes from patients with infertility. As mitochondria and oxidative stress have been postulated to underlie pathogenesis in a wide variety of cells, including oocytes, our method also permits studies of the mechanism by which other maturation failures are increased during meiotic maturation and aging of mammalian oocytes. Further investigation should be carried out to support eventual clinical trials using TPE-Ph-In as an agent to assist IVF. Moreover, TPE-Ph-In might also be used to indicate the increased MMP common in tumor cells or the decreased MMP in apoptotic cells for drug screening.

## Materials and methods

### *Reagents*

Dulbecco's Modified Eagle Medium (DMEM), fetal bovine serum (FBS), and phosphate buffered saline (PBS) were purchased from Hyclone. Penicillin and streptomycin were purchased from Solarbio. $Na_2HPO_4$, citrate acid, and KCl were purchased from Sinoreagent. TPE-Ph-In was kindly donated by AIEgen Biotech. All aqueous solutions for photoluminescence measurements and staining were prepared by adding an aliquot of DMSO stock solution containing 10 mM TPE-Ph-In into the aqueous buffers.

### *Patients*

From April 2019 to May 2019, we recruited 36 male patients from the Reproductive Medical Centre, Renmin Hospital of Wuhan University. Four abandoned oocytes were also obtained from the same institution. All experiments in this study were approved by the Ethic Committee of Life Science of Renmin Hospital, Wuhan University. All experiments were performed in accordance with relevant guidelines and regulations of the Ethic Committee of Life Science of Renmin Hospital of Wuhan University. We received agreement, permission, informed and signed consent from all patients included in the present study. Information regarding the sperm samples from the 36 study participants is summarized in Table S1. The detailed clinical diagnoses of the participants are listed in the supplementary data.

### *Clinical semen analysis*

Semen samples were collected by masturbation after 2-7 days of sexual abstinence. Each semen sample was liquefied for 30 min at 37°C before sample preparations. Manual semen analysis was performed at 37°C within 30 min of collection. The sperm concentration was obtained by counting immobilized sperm with a hemocytometer. The volume, pH, and spermatozoa concentration and motility of the samples were assessed according to World Health Organization guidelines using a computer-assisted semen analyzer (Weili Company, Beijing, China). Motility was estimated on a 37°C microscope stage with the use of a semen wet mount on a covered slide. The motility measurements included the percentage motility,

the percentage of sperm with forward progression, and qualitative assessment of the progressive motility score as: 1, sluggish; 2, slow; 3, good; or 4, vigorous/rapid. Morphology was also assessed.

*Germ cell pretreatment*

Sperm cells were isolated by density gradient centrifugation. SpermGrad with G-IVF PLUS (vitrolife, 10136) was prepared 90% and 45% each in 10 ml, mixed wells and stored in a 15 mL sterile non-toxic centrifuge tube. The two gradients were equilibrated for 0.5 h at 37°C and 6% $CO_2$. Then, 400 μL of the 90% gradient was added to a 1.5 mL conical centrifuge tube, 400 μL of the 45% gradient was slowly added as the upper layer, and finally a 400 μL semen sample was added to the top layer. The sample was centrifuged at 300 *g* at room temperature for 10 min, the two liquid upper layers were carefully removed, and the sperm deposit was transferred to 400 μL equilibrium G-IVF PLUS containing 0.4 μL TPE-Ph-In and 0.4 μL Hoechst 33342. The suspension was then mixed well and allowed to stain at 37°C for 30 min.

The oocytes were washed with DMEM and stained with 500 μL of 10 μM TPE-Ph-In at 37°C for 30 min.

*Sperm physiological detection after staining*

After staining, the physical condition of the sperm, including their general status, activity, and other properties, was observed using an OLYMPUS DMR inverted microscope. The same procedures were also performed on a blank control.

*Cell culture*

HeLa (Cat. No. CCL-2, ATCC) and HCT 116 (Cat. No. CCL-247, ATCC) cells were routinely maintained in DMEM supplemented with 10% FBS and antibiotics (100 units/mL penicillin and 100 g/mL streptomycin) in a 5% $CO_2$ incubator at 37°C.

*Staining of live cells*

One day before the staining experiment, HeLa and HCT 116 cells were seeded into glass-bottom Petri dishes. The cells were cultured in the Petri dishes overnight in DMEM supplemented with 10% FBS without penicillin and streptomycin and then examined by confocal microscopy at approximately 70-80% confluence. As a control, we obtained a semen sample from an individual with normal fertility. We added TPE-Ph-In (1:1,000) to 200 μL semen and tested the sample by flow cytometry. We also performed flow cytometry on a 200 μL sample of semen without TPE-Ph-In staining. For TPE-Ph-In staining, we prepared a 10 mM TPE-Ph-In stock solution in DMSO. Before confocal microscopy, we added the appropriate volume of TPE-Ph-In stock solution directly into the samples. Once the staining was completed, the coverslip with stained live cells was washed twice in 1 × HBSS and examined by confocal microscopy.

We stained live sperm cells with 10 μM TPE-Ph-In in the culture medium. After incubation for 0.5 h at 37°C, we washed the cells three times with PBS. Then, we transferred the cells to medium containing 1 μM Hoechst 33342 and incubated them for 0.5 h. For TPE-Ph-In fluorescence imaging, a 63 × oil immersion objective lens was used with an Argon laser at 40% power to excite the TPE-Ph-In at wavelength = 561 nm. For TPE-Ph-In fluorescence imaging with oocytes, a 20 × oil immersion objective lens was used. A blank sample containing cells without the addition of TPE-Ph-In was used to adjust the emission wavelength, gains, and smart offset so that no autofluorescence was detected under the imaging conditions. The scanning resolution used was 2048 × 2048.

*Cytotoxicity evaluated by MTT assay*

The viability of the cells was determined by MTT assay with absorbance at 560 nm detected using a Thermo Scientific Multiscan FC. Five thousand cells were seeded per well on a 96-well plate. After overnight culture, various concentrations of TPE-Ph-In were added onto the 96-well plate. After 0.5 h, 1 h, or 1.5 h of treatment, 10 μL MTT solution (5 mg/mL in phosphate buffer solution) was added into the each well. After 4 h incubation at 37°C, 150 μL DMSO was added into each well to dissolve the formazan crystals. Complete dissolution was achieved by shaking for 15 min. The absorbance of each well was measured at 560 nm using a plate reader. Four replicate wells were used for each concentration.

*Flow cytometry for fluorescence intensity*

Flow cytometry to measure fluorescence intensity was applied using a BD FACSAria III (USA).

Two milliliters PBS was added to the sperm suspension after staining. The suspension was then filtered and checked on the machine. The instrument was calibrated with non-treated cells (negative control) to identify viable cells, and the cells were then analyzed by a fluorescence scan performed with $1.5 \times 10^6$ cells using the FL1-H channel.

*Multiplexed imaging of patients' sperm samples*

Multiplexed imaging of Hoechst 33342 and TPE-Ph-In signals in live cells was performed using a red channel (TPE-Ph-In) with an excitation wavelength of 488 nm and an emission wavelength of 551-656 nm and a blue channel (Hoechst 33342) with an excitation wavelength of 488 nm and an emission wavelength of 410-501 nm. Patients' sperm cells were stained with 5 μM TPE-Ph-In for 1 h, followed by staining with 1 μM Hoechst 33342 for 10 min. The cells were visualized using a confocal microscope (Zeiss Laser Scanning Confocal Microscope; LSM880) with the ZEN 2009 software (Carl Zeiss). TPE-Ph-In and Hoechst 33342 were excited at 561 nm and 488 488 nm, respectively. The fluorescence was collected at 551-638 nm for TPE-Ph-In and 447-497 nm for Hoechst 33342.

*Photoluminescence measurement*

After pretreatment, the patients' sperm cells were stained with 10 μM TPE-Ph-In for 0.5 h and with 1 μM Hoechst 33342 for 10 min at 37°C. The solutions were then added to Corning S Costar 96-Well Black-Bottom Plates (100 μL/well). Photoluminescence spectra were recorded using the Molecular Devices SpectraMax i3x Multi-ModeMicroplate Detection System.

*Cell counterstaining and colocalization study*

We used MitoTracker Green, a widely used mitochondria-localizing dye, to investigate localization in the mitochondria. We first stained HeLa cells with 10 μM TPE-Ph-In for 0.5 h. Next, we washed the cells twice in PBS, incubated them with 5 μM MitoTracker Green for another 45 min, and washed them twice again. We performed cellular fixation and nuclear staining using conventional procedures. We visualized the counterstained cells using a confocal microscope (Zeiss Laser Scanning Confocal Microscope; LSM880) and the ZEN 2009 software (Carl Zeiss). TPE-Ph-In and Hoechst 33342 were excited at 561 nm and 488 nm, respectively. The fluorescence was collected at 551-638 nm for TPE-Ph-In, 447-497 nm for Hoechst 33342, and 570-630 nm for MitoTracker Green.

*Photostability study of TPE-Ph-In in sperm cells*

We investigated the photostability of TPE-Ph-In using continuous scanning by confocal microscope with the following parameters: Time-Lapse imaging mode, continuous imaging of stained cells at a similar slice, cycling time of 10 s, interval time of 40 s, and total time of cycling of 360 s. We obtained and co-conducted four images of the same channel. The ImageJ software and related plug-ins were used for semi-quantitative analysis of the fluorescence intensity.

*Image analysis*

For confocal imaging of Hoechst 33342, the single-channel raw images were exported in "tiff" format. Using ImageJ, the background of the image from the fluorescence channel was calculated using the "Gaussian Blur", "Minimum Filter", and "Maximum Filter" function and then subtracted from the original image using "image calculator". The background-subtracted image was then subjected to "threshold" setting and "watershed" adjustment before the "analyze particle" function was employed. The results from the "analyze particle" function include the lipid droplet number and size. The data from each image were exported into a spreadsheet for statistical analysis.

For confocal imaging of TPE-Ph-In, the single-channel raw images were exported in "tiff" format. In ImageJ, the "Huang" algorithm was used to set the "threshold" for the exported image of the fluorescence channel, and fluorescence intensity measurement was performed using the "Measure" function. The "Mean gray value" was exported to a spreadsheet for statistical analysis.

*Statistical analysis*

The lipid droplet number, cell size, and MMP intensity values were expressed as the mean

value ± standard deviation (SD). Statistical analysis was performed using an ANOVA for different groups of measurements. Comparisons with $P < 0.05$ were considered to be significant.

## Acknowledgements

We acknowledge Dr Sijie Chen from Ming Wai Lau Centre for Reparative Medicine, Karolinska Institutet, for her kind help in proofreading our manuscript. We are grateful to AIEgen Biotech for their kind donation of TPE-Ph-In. This work is supported by the Key Technologies Research and Development Program (2018YFC03110-05).

## Disclosure of conflict of interest

None.

**Address correspondence to:** Meijia Gu, Key Laboratory of Combinatorial Biosynthesis and Drug Discovery, Ministry of Education, School of Pharmaceutical Sciences, Wuhan University, Wuhan 430071, China. E-mail: mjgu@whu.edu.cn

## References

[1] An international system for human cytogenetic nomenclature (1978) ISCN (1978). Report of the Standing Commitee on Human Cytogenetic Nomenclature. Cytogenet Cell Genet 1978; 21: 309-409.

[2] Loutradi KE, Tarlatzis BC, Goulis DG, Zepiridis L, Pagou T, Chatziioannou E, Grimbizis GF, Papadimas I and Bontis I. The effects of sperm quality on embryo development after intracytoplasmic sperm injection. J Assist Reprod Genet 2006; 23: 69-74.

[3] Tesarik J. Paternal effects on cell division in the human preimplantation embryo. Reprod Biomed Online 2005; 10: 370-375.

[4] Barroso G, Valdespin C, Vega E, Kershenovich R, Avila R, Avendano C and Oehninger S. Developmental sperm contributions: fertilization and beyond. Fertil Steril 2009; 92: 835-848.

[5] Liu DY and Baker HW. Defective sperm-zona pellucida interaction: a major cause of failure of fertilization in clinical in-vitro fertilization. Hum Reprod 2000; 15: 702-708.

[6] Yi XF, Xi HL, Zhang SL and Yang J. Relationship between the positions of cytoplasmic granulation and the oocytes developmental potential in human. Sci Rep 2019; 9: 7215.

[7] Stoop D, Ermini B, Polyzos NP, Haentjens P, De Vos M, Verheyen G and Devroey P. Reproductive potential of a metaphase II oocyte retrieved after ovarian stimulation: an analysis of 23,354 ICSI cycles. Hum Reprod 2012; 27: 2030-2035.

[8] Sanchez T, Wang T, Pedro MV, Zhang M, Esencan E, Sakkas D, Needleman D and Seli E. Metabolic imaging with the use of fluorescence lifetime imaging microscopy (FLIM) accurately detects mitochondrial dysfunction in mouse oocytes. Fertil Steril 2018; 110: 1387-1397.

[9] Toner JP. Progress we can be proud of: U.S. trends in assisted reproduction over the first 20 years. Fertil Steril 2002; 78: 943-950.

[10] Franasiak JM, Forman EJ, Hong KH, Werner MD, Upham KM, Treff NR and Scott RT Jr. The nature of aneuploidy with increasing age of the female partner: a review of 15,169 consecutive trophectoderm biopsies evaluated with comprehensive chromosomal screening. Fertil Steril 2014; 101: 656-663 e651.

[11] Friedman JR and Nunnari J. Mitochondrial form and function. Nature 2014; 505: 335-343.

[12] Galluzzi L, Morselli E, Kepp O, Vitale I, Rigoni A, Vacchelli E, Michaud M, Zischka H, Castedo M and Kroemer G. Mitochondrial gateways to cancer. Mol Aspects Med 2010; 31: 1-20.

[13] Moran M, Moreno-Lastres D, Marin-Buera L, Arenas J, Martin MA and Ugalde C. Mitochondrial respiratory chain dysfunction: implications in neurodegeneration. Free Radic Biol Med 2012; 53: 595-609.

[14] Ong SB and Hausenloy DJ. Mitochondrial morphology and cardiovascular disease. Cardiovasc Res 2010; 88: 16-29.

[15] Chappel S. The role of mitochondria from mature oocyte to viable blastocyst. Obstet Gynecol Int 2013; 2013: 183024.

[16] Bentov Y and Casper RF. The aging oocyte--can mitochondrial function be improved? Fertil Steril 2013; 99: 18-22.

[17] Scheibye-Knudsen M, Fang EF, Croteau DL, Wilson DM 3rd and Bohr VA. Protecting the mitochondrial powerhouse. Trends Cell Biol 2015; 25: 158-170.

[18] Kaneda H, Hayashi J, Takahama S, Taya C, Lindahl KF and Yonekawa H. Elimination of paternal mitochondrial DNA in intraspecific crosses during early mouse embryogenesis. Proc Natl Acad Sci U S A 1995; 92: 4542-4546.

[19] Song MS, Salmena L and Pandolfi PP. The functions and regulation of the PTEN tumour suppressor. Nat Rev Mol Cell Biol 2012; 13: 283-296.

[20] Babayev E and Seli E. Oocyte mitochondrial function and reproduction. Curr Opin Obstet Gynecol 2015; 27: 175-181.

[21] Van Blerkom J, Davis PW and Lee J. ATP content of human oocytes and developmental potential and outcome after in-vitro fertilization and embryo transfer. Hum Reprod 1995; 10: 415-424.
[22] Van Blerkom J. Mitochondrial function in the human oocyte and embryo and their role in developmental competence. Mitochondrion 2011; 11: 797-813.
[23] Krisfalusi M, Miki K, Magyar PL and O'Brien DA. Multiple glycolytic enzymes are tightly bound to the fibrous sheath of mouse spermatozoa. Biol Reprod 2006; 75: 270-278.
[24] Espinoza JA, Schulz MA, Sanchez R and Villegas JV. Integrity of mitochondrial membrane potential reflects human sperm quality. Andrologia 2009; 41: 51-54.
[25] Donnelly ET, O'Connell M, McClure N and Lewis SE. Differences in nuclear DNA fragmentation and mitochondrial integrity of semen and prepared human spermatozoa. Hum Reprod 2000; 15: 1552-1561.
[26] Troiano L, Granata AR, Cossarizza A, Kalashnikova G, Bianchi R, Pini G, Tropea F, Carani C and Franceschi C. Mitochondrial membrane potential and DNA stainability in human sperm cells: a flow cytometry analysis with implications for male infertility. Exp Cell Res 1998; 241: 384-393.
[27] Frank SA and Hurst LD. Mitochondria and male disease. Nature 1996; 383: 224.
[28] Reers M, Smiley ST, Mottola-Hartshorn C, Chen A, Lin M and Chen LB. Mitochondrial membrane potential monitored by JC-1 dye. Methods Enzymol 1995; 260: 406-417.
[29] Scaduto RC Jr and Grotyohann LW. Measurement of mitochondrial membrane potential using fluorescent rhodamine derivatives. Biophys J 1999; 76: 469-477.
[30] Zielonka J, Joseph J, Sikora A, Hardy M, Ouari O, Vasquez-Vivar J, Cheng G, Lopez M and Kalyanaraman B. Mitochondria-targeted triphenylphosphonium-based compounds: syntheses, mechanisms of action, and therapeutic and diagnostic applications. Chem Rev 2017; 117: 10043-10120.
[31] Perry SW, Norman JP, Barbieri J, Brown EB and Gelbard HA. Mitochondrial membrane potential probes and the proton gradient: a practical usage guide. Biotechniques 2011; 50: 98-115.
[32] Luo J, Xie Z, Lam JW, Cheng L, Chen H, Qiu C, Kwok HS, Zhan X, Liu Y, Zhu D and Tang BZ. Aggregation-induced emission of 1-methyl-1,2,3,4,5-pentaphenylsilole. Chem Commun (Camb) 2001; 1740-1741.
[33] Hong Y, Lam JW and Tang BZ. Aggregation-induced emission. Chem Soc Rev 2011; 40: 5361-5388.
[34] Mei J, Leung NL, Kwok RT, Lam JW and Tang BZ. Aggregation-induced emission: together we shine, united we soar! Chem Rev 2015; 115: 11718-11940.
[35] Hong Y, Lam JW and Tang BZ. Aggregation-induced emission: phenomenon, mechanism and applications. Chem Commun (Camb) 2009; 4332-4353.
[36] Cheng Y, Dai J, Sun C, Liu R, Zhai T, Lou X and Xia F. An intracellular $H_2O_2$-responsive AIEgen for the peroxidase-mediated selective imaging and inhibition of inflammatory cells. Angew Chem Int Ed Engl 2018; 57: 3123-3127.
[37] Zhao E, Hong Y, Chen S, Leung CW, Chan CY, Kwok RT, Lam JW and Tang BZ. Highly fluorescent and photostable probe for long-term bacterial viability assay based on aggregation-induced emission. Adv Healthc Mater 2014; 3: 88-96.
[38] Zhao N, Chen S, Hong Y and Tang BZ. A red emitting mitochondria-targeted AIE probe as an indicator for membrane potential and mouse sperm activity. Chem Commun (Camb) 2015; 51: 13599-13602.
[39] Cheng Y, Huang F, Min X, Gao P, Zhang T, Li X, Liu B, Hong Y, Lou X and Xia F. Correction to protease-responsive prodrug with aggregation-induced emission probe for controlled drug delivery and drug release tracking in living cells. Anal Chem 2016; 88: 10773.
[40] Cai Y, Du L, Samedov K, Gu X, Qi F, Sung HHY, Patrick BO, Yan Z, Jiang X, Zhang H, Lam JWY, Williams ID, Lee Phillips D, Qin A and Tang BZ. Deciphering the working mechanism of aggregation-induced emission of tetraphenylethylene derivatives by ultrafast spectroscopy. Chem Sci 2018; 9: 4662-4670.
[41] Zhao N, Yang Z, Lam JW, Sung HH, Xie N, Chen S, Su H, Gao M, Williams ID, Wong KS and Tang BZ. Benzothiazolium-functionalized tetraphenylethene: an AIE luminogen with tunable solid-state emission. Chem Commun (Camb) 2012; 48: 8637-8639.
[42] Wang F, Huang W, Li K, Li A, Gao W and Tang B. Study on the fluorescence enhancement in lanthanum(III)-carminic acid-cetyltrimethylammonium bromide system and its analytical application. Spectrochim Acta A Mol Biomol Spectrosc 2011; 79: 1946-1951.
[43] Gao H, Zhao X and Chen S. AIEgen-based fluorescent nanomaterials: fabrication and biological applications. Molecules 2018; 23.
[44] Chung KM, Lim SU, Hong HJ, Park SY, Park CH, Kim HS, Choi SK and Rew JS. A case of colonic pseudoobstruction related to bacterial overgrowth due to a sigmoidocecal fistula. Korean J Gastroenterol 2014; 63: 125-128.
[45] Richard JA, Massonneau M, Renard PY and Romieu A. 7-hydroxycoumarin-hemicyanine hy-

brids: a new class of far-red emitting fluorogenic dyes. Org Lett 2008; 10: 4175-4178.
[46] Liu F, Wu T, Cao J, Zhang H, Hu M, Sun S, Song F, Fan J, Wang J and Peng X. A novel fluorescent sensor for detection of highly reactive oxygen species, and for imaging such endogenous hROS in the mitochondria of living cells. Analyst 2013; 138: 775-778.
[47] Zhou Y, Hua J, Barritt G, Liu Y, Tang BZ and Tang Y. Live imaging and quantitation of lipid droplets and mitochondrial membrane potential changes with aggregation-induced emission luminogens in an in vitro model of liver steatosis. Chembiochem 2019; 20: 1256-1259.
[48] Gu M, Zeng Z, Wu MY, Leung JK, Zhao E, Wang S and Chen S. Imaging macrophage phagocytosis using aie luminogen-labeled E. coli. Chem Asian J 2019; 14: 775-780.
[49] Yabin Zhou HL, Zhao N, Wang ZM, Michael Z Michael, Xie N, Tang BZ and Tang YH. Multiplexed imaging detection of live cell intracellular changes in early apoptosis with aggregation-induced emission fluorogens. Science China Chemistry 2018; 61.
[50] Dickinson BC and Chang CJ. A targetable fluorescent probe for imaging hydrogen peroxide in the mitochondria of living cells. J Am Chem Soc 2008; 130: 9638-9639.
[51] Xu Z and Xu L. Fluorescent probes for the selective detection of chemical species inside mitochondria. Chem Commun (Camb) 2016; 52: 1094-1119.
[52] Basiji DA, Ortyn WE, Liang L, Venkatachalam V and Morrissey P. Cellular image analysis and imaging by flow cytometry. Clin Lab Med 2007; 27: 653-670, viii.
[53] Caporale T, Ciavardelli D, Di Ilio C, Lanuti P, Drago D and Sensi SL. Ratiometric-pericam-mt, a novel tool to evaluate intramitochondrial zinc. Exp Neurol 2009; 218: 228-234.
[54] Stanley HP and Lambert CC. Differential fate of mitochondria during spermiogenesis in the ratfish hydrolagus. Tissue Cell 1990; 22: 471-476.
[55] Hirata S, Hoshi K, Shoda T and Mabuchi T. Spermatozoon and mitochondrial DNA. Reprod Med Biol 2002; 1: 41-47.
[56] Sousa AP, Amaral A, Baptista M, Tavares R, Caballero Campo P, Caballero Peregrin P, Freitas A, Paiva A, Almeida-Santos T and Ramalho-Santos J. Not all sperm are equal: functional mitochondria characterize a subpopulation of human sperm with better fertilization potential. PLoS One 2011; 6: e18112.
[57] Pena FJ, Saravia F, Johannisson A, Walgren M and Rodriguez-Martinez H. A new and simple method to evaluate early membrane changes in frozen-thawed boar spermatozoa. Int J Androl 2005; 28: 107-114.
[58] Ortega-Ferrusola C, Sotillo-Galan Y, Varela-Fernandez E, Gallardo-Bolanos JM, Muriel A, Gonzalez-Fernandez L, Tapia JA and Pena FJ. Detection of "apoptosis-like" changes during the cryopreservation process in equine sperm. J Androl 2008; 29: 213-221.
[59] Grunewald S, Fitzl G and Springsguth C. Induction of ultra-morphological features of apoptosis in mature and immature sperm. Asian J Androl 2017; 19: 533-537.
[60] Pena FJ, Johannisson A, Wallgren M and Rodriguez-Martinez H. Assessment of fresh and frozen-thawed boar semen using an Annexin-V assay: a new method of evaluating sperm membrane integrity. Theriogenology 2003; 60: 677-689.
[61] Anzar M, He L, Buhr MM, Kroetsch TG and Pauls KP. Sperm apoptosis in fresh and cryopreserved bull semen detected by flow cytometry and its relationship with fertility. Biol Reprod 2002; 66: 354-360.
[62] Vorup-Jensen T, Hjort T, Abraham-Peskir JV, Guttmann P, Jensenius JC, Uggerhoj E and Medenwaldt R. X-ray microscopy of human spermatozoa shows change of mitochondrial morphology after capacitation. Hum Reprod 1999; 14: 880-884.
[63] Courtade M, Lagorce C, Bujan L, Caratero C and Mieusset R. Clinical characteristics and light and transmission electron microscopic sperm defects of infertile men with persistent unexplained asthenozoospermia. Fertil Steril 1998; 70: 297-304.
[64] Wilton LJ, Temple-Smith PD and de Kretser DM. Quantitative ultrastructural analysis of sperm tails reveals flagellar defects associated with persistent asthenozoospermia. Hum Reprod 1992; 7: 510-516.
[65] Gopalkrishnan K, Padwal V, D'Souza S and Shah R. Severe asthenozoospermia: a structural and functional study. Int J Androl 1995; 18 Suppl 1: 67-74.
[66] Piasecka M and Kawiak J. Sperm mitochondria of patients with normal sperm motility and with asthenozoospermia: morphological and functional study. Folia Histochem Cytobiol 2003; 41: 125-139.
[67] Van Blerkom J. Mitochondria in human oogenesis and preimplantation embryogenesis: engines of metabolism, ionic regulation and developmental competence. Reproduction 2004; 128: 269-280.
[68] Nogueira D, Albano C, Adriaenssens T, Cortvrindt R, Bourgain C, Devroey P and Smitz J. Human oocytes reversibly arrested in prophase I by phosphodiesterase type 3 inhibitor in vitro. Biol Reprod 2003; 69: 1042-1052.
[69] Mehlmann LM. Stops and starts in mammalian oocytes: recent advances in understanding the regulation of meiotic arrest and oocyte

maturation. Reproduction 2005; 130: 791-799.
[70] Han SJ, Vaccari S, Nedachi T, Andersen CB, Kovacina KS, Roth RA and Conti M. Protein kinase B/Akt phosphorylation of PDE3A and its role in mammalian oocyte maturation. EMBO J 2006; 25: 5716-5725.
[71] Tosti E. Calcium ion currents mediating oocyte maturation events. Reprod Biol Endocrinol 2006; 4: 26.
[72] McGinnis LK, Carroll DJ and Kinsey WH. Protein tyrosine kinase signaling during oocyte maturation and fertilization. Mol Reprod Dev 2011; 78: 831-845.
[73] Virant-Klun I, Knez K, Tomazevic T and Skutella T. Gene expression profiling of human oocytes developed and matured in vivo or in vitro. Biomed Res Int 2013; 2013: 879489.
[74] Sha W, Xu BZ, Li M, Liu D, Feng HL and Sun QY. Effect of gonadotropins on oocyte maturation in vitro: an animal model. Fertil Steril 2010; 93: 1650-1661.
[75] Liu S, Li Y, Gao X, Yan JH and Chen ZJ. Changes in the distribution of mitochondria before and after in vitro maturation of human oocytes and the effect of in vitro maturation on mitochondria distribution. Fertil Steril 2010; 93: 1550-1555.
[76] Stojkovic M, Machado SA, Stojkovic P, Zakhartchenko V, Hutzler P, Goncalves PB and Wolf E. Mitochondrial distribution and adenosine triphosphate content of bovine oocytes before and after in vitro maturation: correlation with morphological criteria and developmental capacity after in vitro fertilization and culture. Biol Reprod 2001; 64: 904-909.
[77] Sun QY, Wu GM, Lai L, Park KW, Cabot R, Cheong HT, Day BN, Prather RS and Schatten H. Translocation of active mitochondria during pig oocyte maturation, fertilization and early embryo development in vitro. Reproduction 2001; 122: 155-163.
[78] Wilding M, Dale B, Marino M, di Matteo L, Alviggi C, Pisaturo ML, Lombardi L and De Placido G. Mitochondrial aggregation patterns and activity in human oocytes and preimplantation embryos. Hum Reprod 2001; 16: 909-917.
[79] Liu S, Li Y, Feng HL, Yan JH, Li M, Ma SY and Chen ZJ. Dynamic modulation of cytoskeleton during in vitro maturation in human oocytes. Am J Obstet Gynecol 2010; 203: 151, e151-157.
[80] Yu Y, Dumollard R, Rossbach A, Lai FA and Swann K. Redistribution of mitochondria leads to bursts of ATP production during spontaneous mouse oocyte maturation. J Cell Physiol 2010; 224: 672-680.
[81] Ou XH, Li S, Wang ZB, Li M, Quan S, Xing F, Guo L, Chao SB, Chen Z, Liang XW, Hou Y, Schatten H and Sun QY. Maternal insulin resistance causes oxidative stress and mitochondrial dysfunction in mouse oocytes. Hum Reprod 2012; 27: 2130-2145.
[82] Cotterill M, Harris SE, Collado Fernandez E, Lu J, Huntriss JD, Campbell BK and Picton HM. The activity and copy number of mitochondrial DNA in ovine oocytes throughout oogenesis in vivo and during oocyte maturation in vitro. Mol Hum Reprod 2013; 19: 444-450.
[83] Sanchez F, Romero S, De Vos M, Verheyen G and Smitz J. Human cumulus-enclosed germinal vesicle oocytes from early antral follicles reveal heterogeneous cellular and molecular features associated with in vitro maturation capacity. Hum Reprod 2015; 30: 1396-1409.
[84] Liu MH, Zhou WH, Chu DP, Fu L, Sha W and Li Y. Ultrastructural changes and methylation of human oocytes vitrified at the germinal vesicle stage and matured in vitro after thawing. Gynecol Obstet Invest 2017; 82: 252-261.
[85] World Health Organization. DHS comparative reports no 9. WHO. https://www.who.int/reproductivehealth/topics/infertility/DHS-CR9.pdf (September 2004, date last accessed).
[86] Gallon F, Marchetti C, Jouy N and Marchetti P. The functionality of mitochondria differentiates human spermatozoa with high and low fertilizing capability. Fertil Steril 2006; 86: 1526-1530.

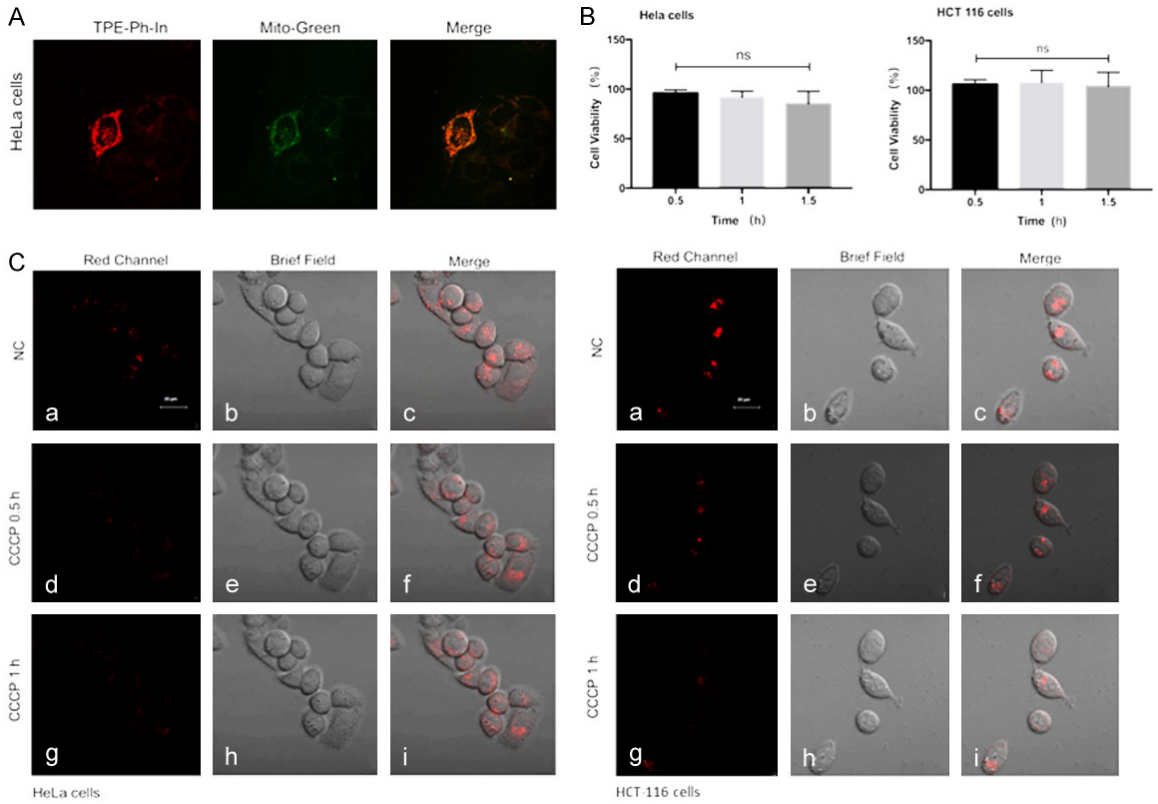


**Figure S1.** Imaging of stained cells and quantification of fluorescence intensity. A. Co-localization of TPE-Ph-In and MitoTracker Green in HeLa cells (excitation wavelength: 561 nm; emission wavelength: red channel 596-663 nm, green channel 478-572 nm). B. Cytotoxicity of TPE-Ph-In evaluated on HeLa and HCT 116 cells by MTT assay at 0.5 h, 1 h, and 1.5 h, each sample with 6 replicates. C. Declining TPE-Ph-In staining intensity indicating changes in mitochondrial membrane potential after carbonyl cyanide 3-chlorophenylhydrazone (CCCP) (20 mM) treatment for used to treat HeLa and HCT 116 cells. The results are from one experiment representative of two similar experiments. (Excitation wavelength: 561 nm; emission wavelength: 596-663 nm). Scale bar = 20 μm. Left: HeLa cells: a-c. HeLa cells stained with TPE-Ph-In (red; photoluminescence = 35.160). d-f. HeLa cells treated with carbonyl cyanide 3-chlorophenylhydrazone CCCP (20 mM) for 0.5 h and then stained with TPE-Ph-In (red). g-i. HeLa cells treated with carbonyl cyanide 3-chlorophenylhydrazone (CCCP) (20 mM) for 1 h and then stained with TPE-Ph-In (red). The membrane potential decreased, and the red fluorescence weakened almost to disappearance (photoluminescence = 7.398). Right: HCT 116 cells: a-c. HCT 116 cells stained with TPE-Ph-In (red; photoluminescence = 50.315). d-f. HCT 116 cells treated with carbonyl cyanide 3-chlorophenylhydrazone CCCP (20 mM) for 0.5 h and then stained with TPE-Ph-In (red). g-i. HCT 116 cells treated with carbonyl cyanide 3-chlorophenylhydrazone CCCP (20 mM) for 1 h and then stained with TPE-Ph-In (red). The membrane potential decreased, and the red fluorescence weakened almost to disappearance (photoluminescence = 8.243).

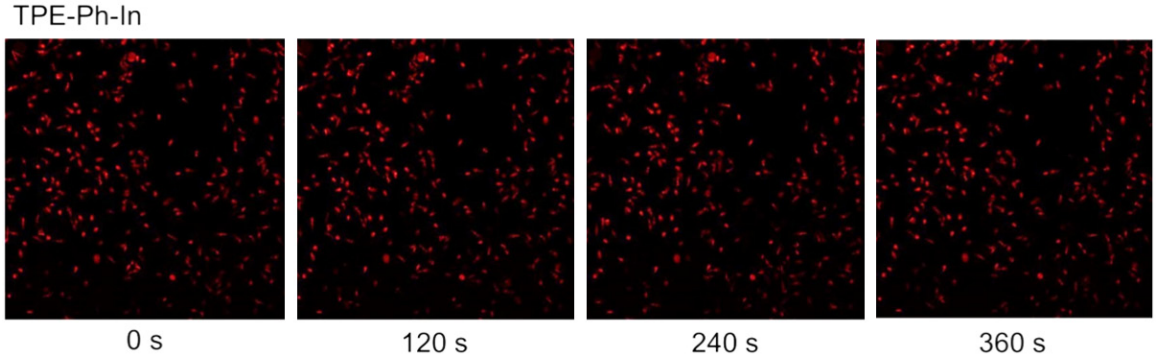


**Figure S2.** Fluorescence images of sperm 0 s, 120 s, 240 s, and 360 s after staining with TPE-Ph-In. Excitation wavelength: 561 nm, emission wavelength: 596-663 nm.

**Table S1.** Sperm characteristics of patients before/after imaging with Tpe-Ph-In

| Sperm | Before | After |
|---|---|---|
| Progressive (PR) motilityin neat semen (%) | 58.5 | 58.6 |
| Non-Progressive (NP) motility in neat semen (%) | 27.7 | 23.5 |
| RP+NP (%) | 85.7 | 82.1 |
| Forward motility (a) (%) | 21.2 | 26.1 |
| Forward motility (b) (%) | 37.3 | 32.5 |

The entire clinical value blow was obtained fromdeo Renmin Hospital of Wuhan University.